

Research Paper

## The Effect of Annealing Temperature on the High Temperature Deformation Behavior of Ti-5Al-4.2V-0.8 Mo-2Fe $\alpha/\beta$ Titanium Alloy

Maryam Morakabati\*, Peyman Ahmadian, Parnia Parvizian

*Faculty of Materials and Manufacturing Technologies, Malek Ashtar University of Technology, Tehran, Iran*

---

### ARTICLE INFO

---

*Article history:*

Received 28 March 2022  
Accepted 6 June 2022  
Available online 1 July 2022

*Keywords:*

*$\alpha/\beta$  titanium alloy  
Mill annealing  
Hot tensile test  
Dynamic globularization  
Dynamic strain aging*

---

### ABSTRACT

---

This paper aims to analyze the effect of annealing temperature on the microstructural changes and the following deformation behavior of Ti-5Al-4.2V-0.8Mo-2Fe  $\alpha/\beta$  titanium alloy at high temperatures. For this purpose, the hot rolled specimens were mill annealed at 700, 750, and 800 °C for 1 hour. The deformation behavior of the milled annealed alloy was assessed using the hot tensile test at the temperature of 750 °C and the strain rate of 0.005 sec<sup>-1</sup>. It was found that, by increasing the mill annealing temperature, the layered microstructure changed to the equiaxed one due to static globularization. After the tensile test, the stress-strain curves showed that by decreasing the annealing temperature from 800 to 700 °C, the peak stress decreased and the elongation increased from 362% to 474%. Moreover, the apparent feature of flow curves suggested yield point phenomena as a result of dynamic strain aging. The maximum elongation of 474% was obtained after mill annealing at 700 °C a finding which is correlated with the promoted fine globular  $\alpha$  phase with the grain size of 4.5  $\mu\text{m}$  and the 44.5% content of the  $\beta$  phase due to the dynamic globularization.

---

**Citation:** Morakabati, M.; Ahmadian, P.; Parvizian, P. (2022). The Effect of Annealing Temperature on the High Temperature Deformation Behavior of Ti-5Al-4.2V-0.8 Mo-2Fe  $\alpha/\beta$  Titanium Alloy, Journal of Advanced Materials and Processing, 10 (3), 27-35. Dor: 20.1001.1.2322388.2022.10.3.3.0

**Copyrights:**

Copyright for this article is retained by the author (s), with publication rights granted to Journal of Advanced Materials and Processing. This is an open – access article distributed under the terms of the Creative Commons Attribution License (<http://creativecommons.org/licenses/by/4.0>), which permits unrestricted use, distribution and reproduction in any medium, provided the original work is properly cited.



---

\* Corresponding Author:

E-Mail: m\_morakabati@mut.ac.ir

## 1. Introduction

Ti-4.5Al-3V-2Mo-2Fe is an  $\alpha+\beta$  titanium alloy that is rich in  $\beta$  phase known as the SP700 alloy. It is attracted for its excellent superplastic properties at a temperature of 700 °C [1]. In addition to the superplastic formability, the fatigue strength and the fracture toughness of SP700 alloy are better than those of other  $\alpha+\beta$  titanium alloys, especially the Ti-6Al-4V alloy [2]. Regarding further  $\beta$  stabilizer solute elements, the  $\beta$ -transus of the SP700 alloy is about 900 °C and its superplastic deformation temperature of it is lower than that of the Ti-6Al-4V alloy [3-5]. The mentioned properties raise the demand for the SP700 alloy in different units of industrial fields such as aerospace [6], medicine, and sports [7-9]. As reported earlier [10, 11], the microstructure of the SP700 alloy is governed significantly by thermomechanical and heat treatment parameters. For instance, regarding the high-temperature deformation of the SP700 alloy, roughing is usually done in the single phase  $\beta$  region, as the  $\beta$  phase has a predominant role in the flow behavior of the alloy and the workability in this region is high. Annealing within the range of 800-840 °C leads to the equiaxed  $\alpha$  and the transformed  $\beta$  phases in the dual phase  $\alpha/\beta$  region [9]. The  $\beta$  phase is also transformed to the Martensite ( $\alpha'$  or  $\alpha''$ ) as a result of being quenched from the  $\alpha+\beta$  region [10]. According to the research [11], the Martensite finish temperature ( $M_f$ ) of the SP700 alloy is lower than the ambient temperature. Therefore, some retained  $\beta$  phases ( $\beta_r$ ) remain in the microstructure of the alloy. Nieh *et al.* [12] reported that the  $\beta_r$  phase in the SP700 alloy is converted to the martensite phase through the stress-induced martensitic transformation resulting in higher strength and excellent formability. In general, the  $\alpha$  phase is harder than the  $\beta$  phase; therefore, the room temperature strength of the SP700 alloy is correlated significantly with the  $\alpha$  phase characteristic [13]. Furthermore, Wang *et al.* [2] demonstrated that the  $\beta$  grains are oriented through the loading direction during the creep test of the SP700 alloy at 500 °C, a finding which is attributed to the excellent creep behavior of the alloy. The superplastic behavior of the SP700 alloy was observed at the fine grain structure ( $d < 10 \mu\text{m}$ ) and the elevated temperature ( $T > 0.5 T_m$ ) [14]. It has been reported [2] that the alloy deforms mainly

by the grain sliding mechanism. Tan [15] analyzed the effect of the strain rate on the superplastic behavior of the SP700 alloy. The results revealed that the sharp declination occurs as the strain rate increases at 700 °C. Moreover, the optimal strain rate at which the alloy shows the superplasticity was approximately achieved at a strain rate of  $10^{-3} \text{ sec}^{-1}$ . Shen *et al.* [16] studied the effect of the competitive dynamic recrystallization (DRX) between  $\alpha$  and  $\beta$  phases on the superplastic behavior of the SP-700 alloy. The results show that the superplasticity of the alloy can be explained by grain boundary sliding (GBS). It has been demonstrated that the rearranged dislocations are converted into high-angle sub-boundaries in  $\alpha$  grains by continuous dynamic recrystallization (CDRX). However, the recrystallized  $\beta$  grains are dominantly induced by discontinuous dynamic recrystallization (DDRX), aided by CDRX. Alabort *et al.* [17] demonstrated that when the subgrain size is greater than the average grain size, GBS is the dominant deformation mechanism of superplasticity, and the accommodation process is dislocation glide. Sheikhalil *et al.* [18, 19] studied the hot compression and hot torsion of the SP-700 alloy, previously. The authors studied the room-temperature mechanical properties of the SP700 alloy by changing heat treatment cycles. Despite comprehensive studies on the mechanical properties of  $\alpha+\beta$  titanium alloys [14-20], the high-temperature deformation properties of the SP700 alloy have not been studied by controlling heat treatment parameters. Therefore, the present work has been undertaken to study the effect of annealing temperature on the hot tensile properties and the microstructure of the Ti-5Al-4.2V-0.8Mo-2Fe alloy. It should be mentioned that changing the annealing temperature resulted in achieving different initial microstructure before deformation.

## 2. Experimental

The chemical composition of the studied alloy characterized in accordance with the optical emission spectroscopy (OES) analysis is shown in Table 1. The composition of the alloy deviated from the chemical composition of the standard SP700 alloy. The  $\beta$  transus temperature of the alloy was measured as  $900 \pm 10 \text{ °C}$  through the annealing quenching technique.

**Table 1.** The chemical composition of the studied alloy by the OES method

Al	V	Mo	Fe	Ti
4.96	4.24	0.78	1.98	Balance

The as-received strip was successfully hot rolled at the single  $\beta$  phase region. The initial hot rolling temperature and reduction were 970 °C and 65 %, respectively. The hot rolling process was performed through five passes, and the thickness of the strip reached from 10 mm to 3.5 mm approximately. After the final hot-rolling pass, the strip was immediately quenched. The diameter and speed of the rollers were 30 cm and 3 rpm, respectively. Afterward, the strip was held at 850 °C for 15 minutes, and hot rolled in order to develop the bi-modal microstructure. The rolling reduction and the number of passes were 40% and 3, respectively. Therefore, the thickness of the strip reached nearly 2 mm. Four specimens with dimensions of  $150 \times 60 \times 2 \text{ mm}^3$  were then cut from the secondary hot-rolled strip. Then, the specimens were mill annealed at 700, 750, and 800 °C for one hour. They were subsequently cooled in the air. The as-annealed specimens were provided with a gauge length of 10 mm and a thickness of 3 mm in accordance with ASTM E2448 [21] for the hot tensile test. The hot tensile test was then conducted at 750 °C and the strain rate of  $5 \times 10^{-3}$  through the Instron 8502 hydraulic machine. In order to analyze the microstructure, the standard metallographic technique was employed. The specimens were mechanically polished with 80-3000 grid SiC paper in water. The chemical etching with a modified Kroll

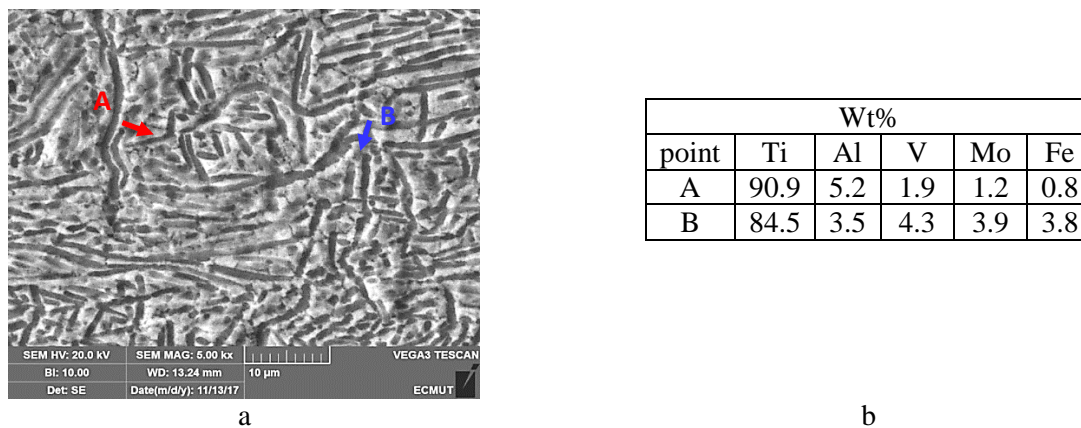
reagent (4 ml HF + 2 ml HNO<sub>3</sub> + 14 ml H<sub>2</sub>O) was employed to reveal the microstructure. The time of etching was between 40 to 60 seconds. Finally, the microstructures of the specimens were evaluated through an Olympus BX 51 optical microscope and a Tescan VEGA3 scanning electron microscope. The grain size and volume fraction of the phases were evaluated quantitatively using the Clemex image analysis software.

### 3. Results and discussion

#### 3.1. Microstructure evolution before deformation

Fig. 1a demonstrates the microstructure of the Ti-5Al-4.2V-0.8Mo-2Fe alloy after the secondary hot rolling process at 850 °C. Fig. 1.b shows the EDS analysis of the points shown in Fig. 1.a. As seen, the enrichment of Al and the depletion of V and Mo contents at point A (the dark area) confirmed the existence of  $\alpha$  phase and vice versa for point B (the light area) which displays the enrichment of V, Mo, and Fe and the depletion of Al contents.

According to Fig. 1a the elongated  $\alpha$  phase is distributed in the  $\beta$  matrix. As a result of dynamic globularization and breaking up lamellar  $\alpha$  phase, a few regions of the globular  $\alpha$  phase have appeared at the prior  $\beta$  matrix.



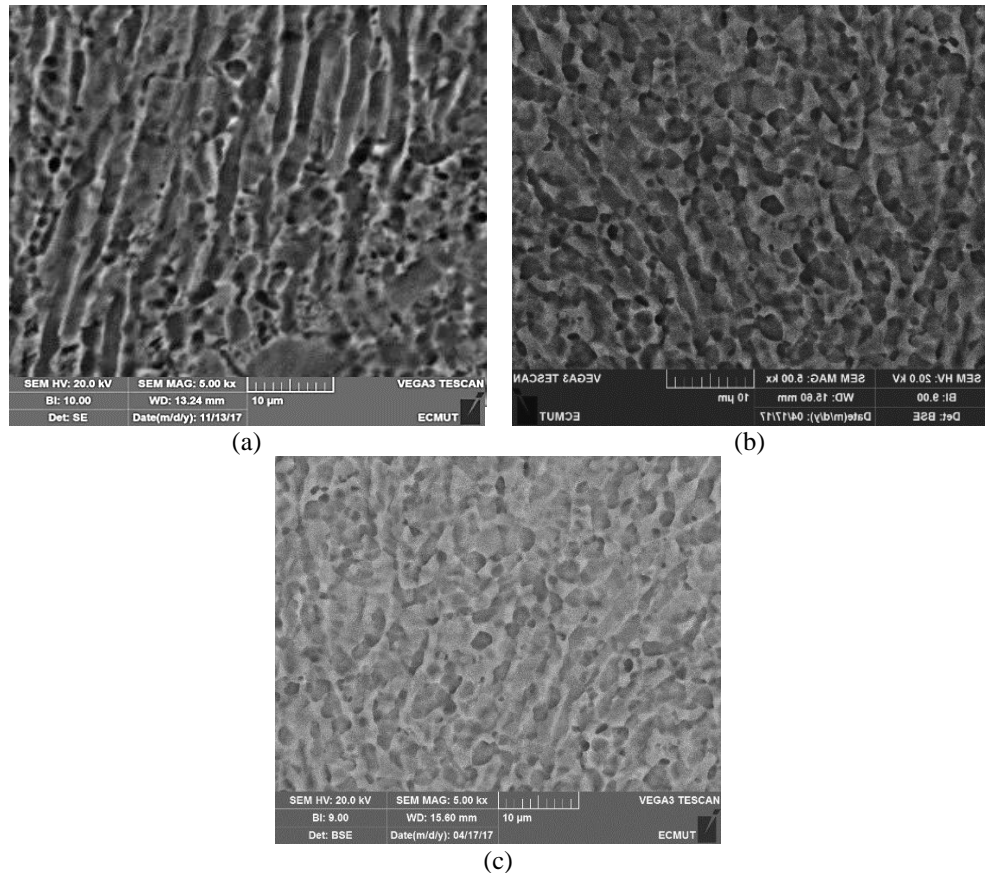
**Fig. 1.** The Scanning Electron Microscopy (SEM) (a) image of the Ti-5Al-4.2V-0.8Mo-2Fe alloy after the secondary hot rolling at 850 °C, and (b) the EDS analysis of points A and B shown in Fig. 1a.

Figure 2 illustrates the SEM images of the specimens after rolling and subsequent mill annealing at 700 to 800 °C. According to Figure 2a, a lamellar morphology of  $\alpha$  phase can be seen in the specimen annealed at 700 °C. In addition, static globularization can be seen in some areas of the microstructure. By increasing the annealing temperature to 750 and 800 °C, the development of static globularization can be observed. As seen, the annealing temperature played an important role in the microstructural characteristics. According to Fig. 2b,c; the evolution of  $\alpha$  lamellar phase, during static globularization and

kinking was a prevailing microstructure feature at temperatures of 750 and 800 °C. As seen in Fig. 2, the degree of static globularization of  $\alpha$ -lamellae increased with an increase in the temperature, while the lamellae became coarser and their aspect ratio decreased. Indeed, by increasing temperature, the migration of interfaces is facilitated due to powerful diffusional effect of accelerating globularization process of lamellae and accordingly increasing the globularized fraction. The similar findings have been reported previously for globularization of Ti6242 alloy [22]. As reported [23], the globularization

involves two steps: 1) boundary segregation and 2) boundary migration. During these steps, the  $\alpha/\alpha$  interface is eliminated, and the globularization process is completed. The second step of

globularization (*i.e.*, boundary migration) is a diffusion-dependent process [24, 25]; therefore, increasing the annealing temperature resulted in a high-volume fraction of the globular  $\alpha$  phase.



**Fig. 2.** The scanning electron microscopy (SEM) images of the alloy after the mill annealing treatment at different temperatures of (a) 700 °C, (b) 750 °C, and (c) 800 °C for one hour.

### 3.2. High deformation properties

Figure 3a depicts the flow stress curve of the alloy annealed at temperatures of 700, 750, and 800 °C after the hot tensile test at 750 °C and the constant strain rate of 0.005 sec<sup>-1</sup>. The flow stress curve of all mill annealed specimens revealed strain hardening in

the first step of deformation due to the generation and multiplication of dislocations. The flow stress increased to peak stress as the plastic strain increased. Subsequently, its value decreased until fracture. Moreover, the flow stress decreased, and the ductility enhanced from 362% to 474% as the mill annealing temperature decreased.

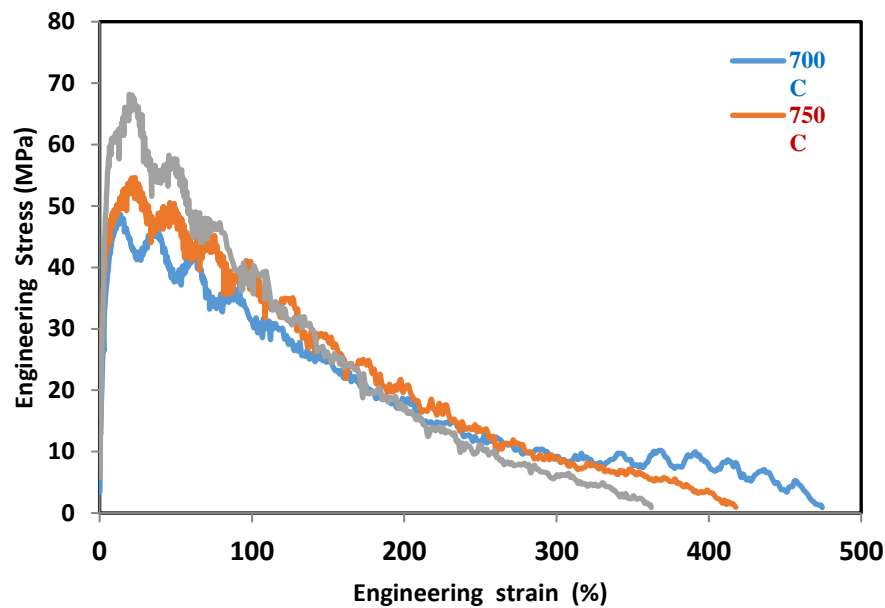


**Fig. 3.** The effect of the mill annealing temperature on the flow stress curve of the alloy during the hot tensile test at 750 °C with the constant strain rate of 0.005 sec<sup>-1</sup>

I

In Figure 3, some serrations can be seen in the flow curves. This behavior is designated as the yield point phenomenon which is attributed to dynamic strain aging. According to references [26, 27], as the interstitial and substitutional solute atoms pin the pre-existing dislocations, the immobile dislocations increased abruptly the yield stress resulted in the appearance of the upper point ( $\sigma_U$ ). This activates new sources of dislocations. When dislocations start to move, the flow stress suddenly decreases resulting to lower yield point ( $\sigma_L$ ) leading to the appearance of serration in the flow curves.

According to Figure 3, the elongation value of the specimen annealed at 700 °C was obtained as 474%. However, at higher mill annealing temperatures, a drop in the elongation of the alloy was observed. The elongation values of the specimens annealed at 750 and 800 °C were measured as 417% and 362%, respectively. Hence, it was found that the highest elongation was achieved for the specimen mill annealed at 700 °C.

### 3.3. Microstructure Evolutional after Superplastic Deformation

Figure 4 shows the microstructure of the specimens after the hot tensile test. For all the specimens, the metallographic images were captured from a severely deformed zone, the tip region. According to the SEM images, after the deformation, the microstructure of the specimen mill annealed at 700 °C, includes the refined globular  $\alpha$  phase surrounded by the  $\beta$  matrix. A similar microstructure can be seen for the specimens annealed at 750 and 800 °C, as well. When the strain is applied to a titanium alloy, the globular phase is required to reduce the free energy of the

deformed material. Therefore, dynamic globularization occurs. The mechanism of dynamic globularization is similar to static globularization; though the plastic deformation is added to temperature leading to dynamic restoration phenomena.

Table 2 shows the effect of the mill annealing temperature on the microstructural characterization of the alloy before and after the deformation at 750 °C. Evidently, the grain size of the  $\alpha$  phase of the deformed specimens was smaller than that of the mill-annealed ones. According to Table 2, the grain size of the  $\alpha$  phase at the deformed region of the specimens annealed at 700, 750, and 800 °C were determined as 12.4, 9.2, and 7.8  $\mu\text{m}$ , respectively. As seen, the maximum change in the grain size is obtained for the specimen mill annealed at 700 °C. The lamellar  $\alpha$  phase in the specimen mill annealed at 700 °C, is favorable for dynamic globularization rather than the lamellar and globularized  $\alpha$  phase. As the dislocation density of the lamellar structure is higher than the globularized structure, the stored energy of the prior one is higher than the subsequent one. Thus, the finer globularized  $\alpha$  phase would be evaluated for the specimen mill annealed at 700 °C by the acceleration of dynamic globularization. Since the finer grains resulted in more  $\alpha/\beta$  grain boundaries, the number of active slip systems increased. Consequently, grain boundary sliding facilitated leading to an increase in elongation during the hot tensile test. Hence, the finer grain size of the  $\alpha$  phase in the specimen annealed at 700 °C in comparison with 750 and 800 °C after deformation, is one of the main reasons for the highest elongation of 474% achieved for the former one. As mentioned before, the increase in grain size of the  $\alpha$  phase in the

deformed specimens can be seen by increasing the mill annealing temperature. The increase in grain size by raising the annealing temperature to 800 °C

restricts grain boundary sliding leading to lower elongation.

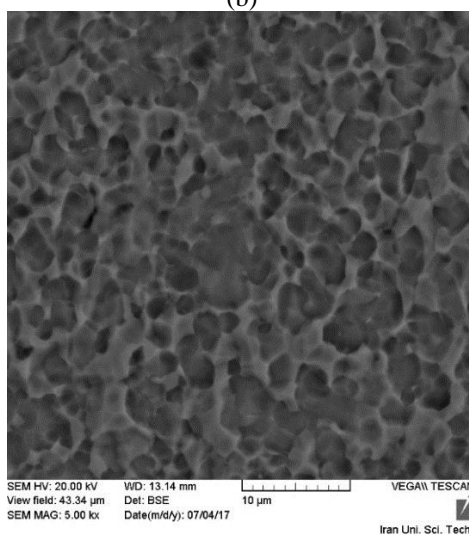
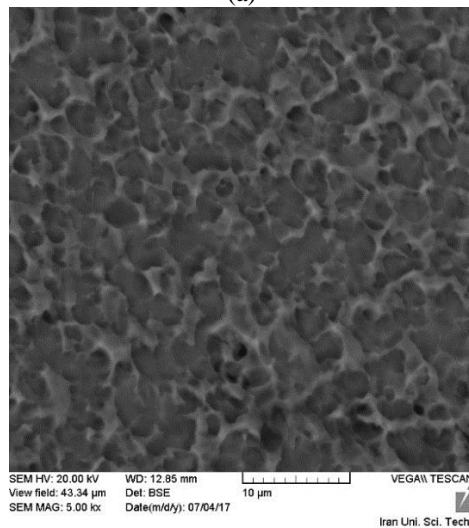
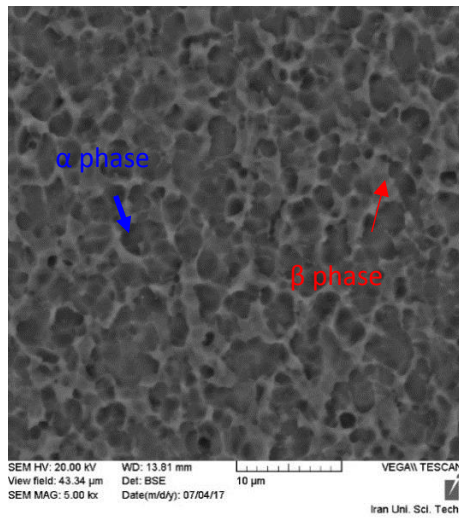


**Fig. 4.** Scanning electron microscopy images of the specimen's mill-annealed at different temperatures of a) 700 °C; b) 750 °C; and c) 800 °C after the hot tensile test at 750 °C with the strain rate of 0.005 sec<sup>-1</sup>

**Table 2.** The effects of the mill annealing temperatures on the microstructural characteristics of the alloy before and after the deformation at 750 °C

Annealing Temperature (°C)	Before Deformation		After Deformation	
	grain size of $\alpha$ phase ( $\mu\text{m}$ )	Volume fraction of $\beta$ phase	grain size of $\alpha$ phase ( $\mu\text{m}$ )	Volume fraction of $\beta$ phase
700	12.4	42.3	4.5	44.5
750	9.2	45.9	5.2	47.2
800	7.8	53.1	6.7	55.3

The morphology of grains is another parameter that can significantly affect the superplastic behavior of titanium alloys. As a result of globular grains, the grain boundary sliding is facilitated. However, the grain boundary sliding through the deformation direction is restricted in wide and elongated grains. The shear stress is not developed appropriately in elongated grains. The induced shear stress during the grain boundary sliding is endured with globular grains. Therefore, it is necessary to develop equiaxed and globular grains for grain boundary sliding during superplastic deformation. According to Figure 4, the globular  $\alpha$  phase was promoted as a result of dynamic globularization. For instance, the initial microstructure of the alloy after annealing at 700 °C (Figure 2a) was compared with its newly promoted microstructure after the deformation (Figure 4a). As mentioned before, the elongated  $\alpha$  phase was broken during the deformation, and globular grains were achieved. Accordingly, the equiaxed and globular grains achieved for the specimen mill annealed at 700 °C confirmed the maximum elongation of 474%.

The volume fraction of the  $\alpha$  and  $\beta$  phases has also a significant effect on the superplastic behavior of titanium alloys. The volume fraction of the  $\beta$  phase of the alloy before and after the hot tensile test has been also demonstrated in Table 2. Evidently, the volume fraction of the  $\beta$  phase of the undeformed specimens increased from 42.3% to 53.1% by increasing the mill-annealing temperature. The volume fraction of the  $\beta$  phase after deformation increased from 44.5% to 55.3%, as well. Due to the different crystal structures of  $\alpha$  and  $\beta$  phases, the superplastic behavior of these two phases is totally different. There are fewer active slip systems in the  $\alpha$  phase with the HCP structure than in the  $\beta$  phase with the BCC structure. Therefore, the self-diffusion rate of the  $\alpha$  phase is twice smaller than that of the  $\beta$  phase. Thus, the  $\alpha$  phase is considerably harder than the  $\beta$  phase at the same temperature and the same strain rate in the superplastic region. As the volume fraction of the  $\beta$  phase increases, stress relaxation occurs easily in the grain boundary sliding process. Eventually, the superplastic properties are enhanced.

It has been reported that [28] the secondary phase has positive effects on the sliding of grain boundary (*i.e.*,  $\alpha/\alpha$  and  $\beta/\beta$  boundaries) and phase boundary ( $\alpha/\beta$  boundaries). As a result of increasing the volume fraction of the  $\beta$  phase, the  $\alpha/\alpha$  grain boundaries were diminished, and the deformation mechanism was controlled predominantly by  $\alpha/\beta$  sliding. Consequently, the higher volume fraction of  $\alpha/\beta$  boundaries is correlated with an excellent elongation value obtained from the superplastic deformation. According to the findings [29,30], the excellent superplastic behavior of the dual-phase titanium alloys was observed when the volume fraction of the  $\beta$  phase is within the range of 40–50%. The optimum volume fraction of the  $\beta$  phase can be observed for the specimen mill-annealed at 700 °C. Consequently, an appropriate volume fraction of the  $\alpha$  phase decreases the grain growth rate of the  $\beta$  phase significantly. Because the best incoherent interface of  $\alpha/\beta$  phases is obtained in the alloy. In this condition, the content of the grain boundary sliding at an incoherent interface (*i.e.*,  $\alpha/\beta$ ) is greater than that of a coherent one (*i.e.*,  $\alpha/\alpha$  or  $\beta/\beta$ ). For the specimen's mill-annealed at 750 °C and 800 °C, the higher volume fraction of the  $\beta$  phase can be observed. As known, the growth rate of the grains in the titanium alloys with the excessive volume fraction of the  $\beta$  phase is high. Moreover, the high diffusion coefficient of the  $\beta$  phase leads to rapid grain growth. Consequently, it can be concluded the grain boundary sliding is suppressed in the specimen's mill-annealed at 750 °C and 800 °C. Therefore, the maximum elongation of 474 % obtained for the specimen mill-annealed at 700 °C with the minimum globular  $\alpha$  grain size and the 44.5 volume fraction of  $\beta$  phase.

#### 4. Conclusion

1. By increasing the mill annealing temperature from 750 and 800 °C, the lamellar  $\alpha$  phase transformed into the globular one by static globularization.
2. The flow curve of all mill annealed specimens revealed strain hardening in the first step of deformation up to peak stress and subsequently softening until fracture.

3. The elongation of the alloy decreased from 474 to 362 % as the mill annealing temperature increased from 700 to 800 °C.
4. During the deformation of the Ti-5Al-4.2V-0.8Mo-2Fe alloy, the flow curves were serrated which is attributed to yield point phenomena as a result of dynamic strain aging.
5. The microstructural evaluation of the mill annealed specimens deformed at 750 °C showed the appearance of a fine globular  $\alpha$  phase as a consequence of dynamic globularization of the lamellar  $\alpha$  phase.
6. The maximum elongation of 474% was obtained for the specimen mill-annealed at a temperature of 700 °C with the 4.5  $\mu\text{m}$  fine globular  $\alpha$  phase and 44.5% volume fraction of the  $\beta$  phase.

## References

- [1] A. Ogawa, H. Fukai, K. Minakawa, and C. Ouchi, "SP-700 Titanium Alloy Data Sheets, Beta titanium alloys in the 1990's", Proc. Annual meeting of the Minerals, Metals and Materials Society (TMS); Denver, CO (United States, Warrendale, p.513.
- [2] W. Shing-Hoa, L. Hao-Hsun, Ch. Chih-Yuan, Y. Jer-Ren, and K. Chin-Hai, "The variation of  $\beta$  phase morphology after creep and negative creep for duplex titanium alloys", J. Mater. Sci., Vol. 44, 2009, pp.408-413.
- [3] C. Leyens, M. Peters, Titanium and titanium alloys fundamental and applications, Weinheim, Wiley-VCH Verlag, Germany, 2004, p. 49.
- [4] E.W. Collings, Materials properties handbook: titanium alloys, Materials Park, ASM International, Ohio, 1994 p. 68.
- [5] C. Ouchi, K. Minakawa, K. Takahashi, A. Ogawa, M. Ishikawa, Development of  $\beta$ -rich  $\alpha + \beta$  Titanium Alloy SP-700, NKK Tech. Review, 1992.
- [6] J. Williams, and R. R. Boyer, "Opportunities and issues in the application of titanium alloys for aerospace components", Metals, Vol. 10, no. 6, 2020, pp. 705.
- [7] A. Ogawa, M. Niikura, C. Ouchi, K. Minakawa, M. Yamada, "Development and applications of titanium alloy SP-700 with high formability", J. Test. Evalu., Vol. 24, No. 2, 1996, pp. 100-109.
- [8] K. V., Sudhakar, and E. Wood, "Superplastic grade titanium alloy: comparative evaluation of mechanical properties, microstructure, and fracture behavior", J. Mater., Vol. 11, 2016, pp.1-7.
- [9] Y. B. Lee, D. H. Shin, K-T. Park, and W. J. Nam, "Effect of annealing temperature on microstructures and mechanical properties of a 5083 Al alloy deformed at cryogenic temperature", Scripta Mater., Vol. 51, 2004, pp. 355-359.
- [10] J-K. Nieh, C-T. Wu, Y-L. Chen, Ch-N. Wei, and Sh-L. Lee, "Effect of cooling rate during solution heat treatment on the microstructure and mechanical properties of SP-700 titanium alloys", J. Mari. Sci. Tech., Vol. 24, No. 2, 2016, pp. 99-106.
- [11] C. R. Brooks, Heat treatment, structure and properties of nonferrous alloys, Metals Park, ASM, Ohio, 1982 p. 115.
- [12] J. K. Nieh, Sh-L. Lee, and K-S. Pan, "Effect of heat treatment and deformation on the microstructure and mechanical properties of SP-700 titanium alloy", Inter. J. Mater. Res., Vol. 106, No. 12, 2015, pp. 1224-1229.
- [13] Y. L. Kao, G. C. Tu, C. A. Huang, and T. T. Liu, "A study on the hardness variation of  $\alpha$ - and  $\beta$ -pure titanium with different grain sizes", Mat. Sci. Eng. A, Vol. 398, No. 1-2, 2005, pp. 93-98.
- [14] A. Ogawa, H. Iizumi, "Superplasticity and post-spf properties of SP-700" Proc. The conference Titanium '95: science and technology, vol I, Birmingham, UK, 1995, p. 588.
- [15] S. F. Tan, M.J. Hie, "High Temperature Deformation of Titanium SP-700", Proc. The conference Ti-2007 Science and Technology, The Japan Institute of Metals, Japan, 2007, p. 567.
- [16] J. Shen, Y. Sun, Y. Ning, H. Yu, Z. Yao and L. Hu "Superplasticity induced by the competitive DRX between BCC beta and HCP alpha in Ti-4Al-3V-2Mo-2Fe alloy", Mat. Char., Vol. 153, 2019, 304-317.
- [17] E. Alabort, P. Kontis, D. Barba, K. Dragnevski and R.C. Reed "On the mechanisms of superplasticity in Ti-6Al-4V", Acta Mater., Vol. 105, 2016, 449-463.
- [18] A.H. Sheikhal, M. Morakabati and S.M. Abbasi "Hot torsion behavior of SP-700 near beta titanium alloy in single and dual phase regions", Inter. J. Mater. Res., Vol. 109, 2018, 1136-1145.
- [19] Sheikhal AH and Morakabati M " Hot working of SP-700 titanium alloy with lamellar  $\alpha + \beta$  starting structure using a processing map", Inter. J. Mater. Res., Vol. 111, 2020 (4), 297-306.
- [20] P. Parvizian, M. Morakabati, and S. Sadeghpour, "Effect of hot rolling and annealing temperatures on the microstructure and mechanical properties of SP-700 alloy", Inter. J. Min., Metall. Mat., Vol. 27, 2020, pp. 374-383.
- [21] Standard Test Method for Determining the Superplastic Properties of Metallic Sheet Materials," ASTM E2448, 2011.
- [22] Hot working behavior of near alpha titanium alloy analyzed by mechanical testing and processing map, Maryam Morakabati, Alireza Hajari, Transactions of Nonferrous Metals Society of China, 30, 1560-1573, 2022.
- [23] F. Humphreys, and M. Hatherly Recrystallization and related annealing phenomena. 2nd ed, Oxford: Elsevier, England, 2004, p. 457.



- [24] C. H. Park, J. W. Won, J.-W. Park, S. Semiatin, and C. S. Lee, "Mechanisms and kinetics of static spheroidization of hot-worked Ti-6Al-2Sn-4Zr-2Mo-0.1 Si with a lamellar microstructure", *Metall. Mater. Trans. A*, Vol. 43, 2012, pp. 977-985.
- [25] S. Semiatin, N. Stefansson, and R. Doherty, "Prediction of the kinetics of static globularization of Ti-6Al-4V", *Metall. Mater. Trans. A*, Vol. 36, 2005, pp. 1372-1376.
- [26] P. Wanjara, M. Jahazi, H. Monajati, S. Yue, J.-P. Immarigeon, "Hot working behavior of near- $\alpha$  alloy IMI834", *Mater. Sci. Eng. A*, Vol. 396, 2005, pp. 50-60.
- [27] I. Philippart, H. J. Rack, "High temperature dynamic yielding in metastable Ti-6.8Mo-4.5F-1.5Al", *Mater. Sci. Eng. A*, Vol. 243, 1998, pp. 196-200.
- [28] Du, Z., Liu, J., Li, G., Lv, K., Yan L., Chen, Y., "Low-temperature superplastic behavior of  $\beta$  titanium alloy", *Mater. Sci. Eng. A*, 2016, vol. 650, pp. 414-421.
- [29] A.K.M. Nurul Amin, *Titanium alloys- towards achieving enhanced properties for diversified applications: IntechOpen*, 2012, 1st ed, p. 145.
- [30] X. Zhang, L. Cao, Y. Zhao, Y. Chen, X. Tian, and J. Deng, "Superplastic behavior and deformation mechanism of Ti600 alloy", *Mater. Sci. Eng. A*, 2013, vol. 560, pp. 700-704.